Micro- and macroscopic observations of the nucleation process and crystal growth of nanosized Cs-pollucite in an organotemplate-free hydrosol

Eng-Poh Ng, Aleid Ghadah Mohammad S, Séverinne Rigolet, T. Jean Daou, Svetlana Mintova, Tau Chuan Ling

NJC

PAPER

View Article Online
View Journal

Cite this:

Micro- and Macroscopic Observations of the Nucleation Process and Crystal Growth of Nanosized Cs-Pollucite in Organotemplate-free Hydrosol

Eng-Poh Ng,[a,†] Aleid Ghadah Mohammad S,[a,b] Severinne Rigolet,[c,d] T. Jean Daou,[c,d] Svetlana Mintova,[e,f] Tau Chuan Ling[g]

The nucleation and crystal growth of nanoscale cesium pollucite aluminosilicate zeolite (ANA topology) from an organotemplate-free precursor suspension are reported. By using a new and reactive synthesis recipe ($5.5SiO_2$:$1Al_2O_3$:$6Cs_2O$:$140H_2O$), zeolite nanocrystals with higher Al content (Si/Al ratio = 2.12) are obtained within 120 min under mild condition (180 °C) which is much faster and safer as compared to those previously reported. The solid initially experiences amorphous phase re-organization before nucleation, crystallization and crystal growth take place. The resulting Cs-pollucite nanocrystals (average size 55 nm) display trapezohedron morphology. The nanocrystals are colloidally stabilized in water and they are very active in base-catalyzed cyanoethylation of dipropylamine reaction, giving 89.6% conversion at 180 °C within 50 min. In addition, high solid yield of nanocrystals (ca. 70%) is also achieved, thus offering a green pathway for synthesizing zeolite nanocrystals with high basicity in large scale.

Introduction

Zeolites are crystalline microporous minerals composed of aluminate and silicate tetrahedral units. These molecular sieves are generally used in adsorption, ion-exchange and catalysis owing to their high ion exchange capacity and porosity, and unique framework structure.[1–5] In recent years, decreasing the scale of crystallite size of zeolites to nanometer regime (<100 nm) has attracted immense research interest because of their exceptional properties (e.g. high external surface area, fast diffusivity, high surface charge density, high colloidal stability, etc.) and greater potentiality that is directly related to their particle size.[6–9] Up to now, more than 240 types of zeolite frameworks have been synthesized with only about 20 types of zeolites and related microporous materials can be obtained in nanocrystal forms (ABW,[10] AEI,[11] AFI,[12] AFO,[13] ANA,[14] *BEA,[15] CHA,[16] EDI,[7] EMT,[17] FAU,[18,19] GIS,[20] LTA,[21] LTJ,[22] LTL,[23] MEL,[24] MER,[25] MFI,[26,27] MOR,[28] SOD[29]).

[a]School of Chemical Sciences, Universiti Sains Malaysia, 11800 USM, Penang, Malaysia. Email: epng@usm.my
[b]Department of Chemistry (Preparatory Year), Faculty of Science, University of Hail, P.O. Box 2440, Hail, Kingdom of Saudi Arabia.
[c]Université de Haute-Alsace, Axe Matériaux à Porosités Contrôlées, Institut de Science de Matériaux de Mulhouse UMR 7361, ENSCMu, 3b rue Alfred Werner, 68093 Mulhouse, France.
[d]Université de Strasbourg, 67000 Strasbourg, France.
[e]Laboratoire Catalyse & Spectrochimie, ENSICAEN, Université de Caen, 14000 Caen, France.
[f]State Key Laboratory of Heavy Oil Processing, College of Chemical Engineering, China University of Petroleum (East China), Qingdao, 266580, China.
[g]Institute of Biological Sciences, Faculty of Science, University of Malaya, 50603 Kuala Lumpur, Malaysia.

Cs-pollucite ($CsAlSi_2O_6$) is a rare alkali metal zeolite. It has three-dimensional channel with 8-membered ring pore size (pore opening 2.43 Å) forming ANA framework structure.[30] Cs-pollucite has recently been reported as a promising basic catalyst and host for storing radioactive cesium.[31] In general, the synthesis of Cs-pollucite involves hydrothermal treatment at high temperature (200–300 °C) and pressure (300–850 bar) where natural zeolite[31] and soil[32] are used as aluminosilicate sources. Its synthesis condition which uses high pressure and temperature, however, is considerably dangerous and proper reaction vessels with safety build in have to be employed.

The synthesis of nanosized zeolites requires a specific environment called supersaturation where such conditions allow control of the ultimate crystal size *via* nucleation process. In order to achieve this condition, harmful and costly organic templates in large excess amount are needed which makes the industrial scale-up process to be unfeasible and environment-unfriendly.[21] Hence, fast crystallization of Cs-pollucite nanocrystals under very mild (low pressure and temperature) and eco-friendly (organotemplate-free) condition is still a great challenge in zeolite research.

In this paper, the induction, nucleation and crystal growth of Cs-pollucite zeolite nanocrystals in the organotemplate-free precursor suspension are reported. Unlike previous work,[31,32] the formation evolution of zeolite is studied using a very reactive hydrosol under microscopy and spectroscopy where the crystallization time is significantly reduced from hours to minutes.

Experimental Section

Synthesis of Cs-pollucite zeolite nanocrystals

Initially, cesium hydroxide monohydrate (10.500 g, 99.5%, Sigma-Aldrich), aluminum hydroxide (1.242 g, extra pure, Acros) and distilled water (8.063 g) were stirred at 105 °C for 18 h until a clear solution was obtained. A clear silicate solution was prepared by dissolving HS-40 (6.581 g, 40% SiO_2, Sigma-Aldrich) and cesium hydroxide monohydrate (5.550 g) into distilled water (6.400 g). Then, the aluminate solution was slowly mixed into to the silicate solution under magnetic stirring (450 rpm). A clear precursor suspension with a chemical composition of $5.5SiO_2$:$1Al_2O_3$:$6Cs_2O$:$140H_2O$ was obtained. The precursor solution was transferred into an autoclave and heated at 180 °C for 120 min before the solid product was separated, purified using high-speed centrifugation (10000 rpm, 8 min) and freeze-dried. The samples heated at different time intervals (10, 25, 30, 45 and 60 min) were also prepared following the same procedure.

Characterization

The solid products were analyzed by using a PANalytical X'Pert PRO XRD instrument system with CuKα radiation (λ = 1.5406 Å). The degree of crystallinity was computed by comparing the intensity of the three most important peaks at 24.3°, 26.1° and 30.7° of Cs-pollucite sample (120 min) as 100% crystalline. The average sizes of zeolite crystals were estimated by using the Scherrer equation. TEM images of amorphous, semi-crystalline and crystalline solids were recorded using a Philips CM12 transmission electron microscope operating at 200 kV. The average crystal sizes of zeolites were also estimated using the Image J software by randomly selecting the 50 particles through TEM images. The functional groups of the solids were identified by Fourier Transform Infrared spectroscopy (FTIR) using a Perkin Elmer's System 2000 spectrometer in the wavenumber range of 400-4000 cm-1 (KBr: sample ratio = 50:1). The composition, or Si/Al ratio, of the solids was measured by using ICP-OES spectrometry (Vista MPX, Varian Inc.). Prior to analysis, the solid was first dissolved in a 0.5 M HF solution where boric acid was also added to minimize interferences of fluoride during the analysis. The ^{29}Si MAS NMR spectroscopy measurement was performed using a Bruker Avance II 400 MHz spectrometer system (9.4 Tesla). The sample powder was packed into a 4 mm ZrO_2 rotor and spun at 12 kHz. The chemical shifts were referred to TMS. A single pulse excitation was applied with a $\pi/6$ length of 2.1 µs, a recycle delay of 80s, accumulated during 2000 scans.[33] The ^{27}Al MAS NMR spectra were recorded using different configurations (9.4 Tesla; rotor 2.5 mm; 50000 scans; p/12 rf pulse length of 0.7 ms; recycle delay of 1 s; spinning rate 25 kHz). The chemical shifts was referred to external $[Al(H_2O)_6]^{3+}$ in $AlCl_3$ aqueous solution.

Catalytic reaction study in cyanoethylation of amines

Initially, dried Cs-ABW (0.50 g, 100 °C, 6 h), acrylonitrile (19 mmol, 99%, Merck) and dipropylamine (76 mmol, 99%, Merck) were mixed in a quartz tube (10 mL). The tube was sealed with a silicone cap and subjected to instant heating using a Monowave 50 non-microwave instant heating reactor (Anton Paar) at 180 °C for specific time periods. The resulting reaction solutions after being isolated from the solid catalyst were injected into a GC-FID (Agilent 7890A) and a GC-MS (Agilent 7000 Series Triple Quad GC/MS) instruments for chromatography identification purpose where toluene was used as an internal standard. For the reactions using NaOH and KOH as the catalysts, 1.984 mmol of hydroxide, which is equivalent to 0.50 g of nanosized Cs-pollucite, was used.

Results and discussion

Macroscopic study of the formation of nanosized Cs-pollucite

The kinetics of the formation of Cs-pollucite nanozeolite from a clear precursor solution was initiated by mixing both the silicate and aluminate solutions. The solution was subjected to hydrothermal treatment at 180 °C for 7 min. It was found that the precursor remained clear and no solid product was recovered. However, it turned to cloudy after 15 min of heating. A soft gel was separated upon centrifugation and an amorphous solid with 15.70% yield was collected after purification and freeze-drying (Figures 1–3). As seen from the TEM image, the amorphous solid exhibited thin sheet like structure (Figure 4a).

A soft gel was still obtained with heating time extended to 25 min. At this stage, the solid yield significantly dropped to 8.45%. According to XRD analysis, the sample was still amorphous, but the amorphous hump at 2θ = 18–30° has shifted to 2θ = 24–33° (Figure 2b). The TEM image showed that morphological change of amorphous solid occurred where the amorphous entities (ca. 15 nm) with irregular shape was formed (Figure 4b). The solid yield increased gradually to 21.26% upon heating to 30 min. At this time, several diffraction peaks slowly appeared at 2θ = 24.3° [321], 26.1° [400], 30.7° [332] and 37.2° [440] while the amorphous phase was still dominant (17.78% crystallinity) (Figures 1–3). Thus, it revealed the formation of Cs-pollucite nuclei in this sample. The XRD investigation was further supported by TEM study where crystalline particles (ca. 21 nm) embedded in the amorphous solid were observed (Figure 4c). As seen, the semi-crystalline nuclei had nearly identical crystallite size as the amorphous single particles.

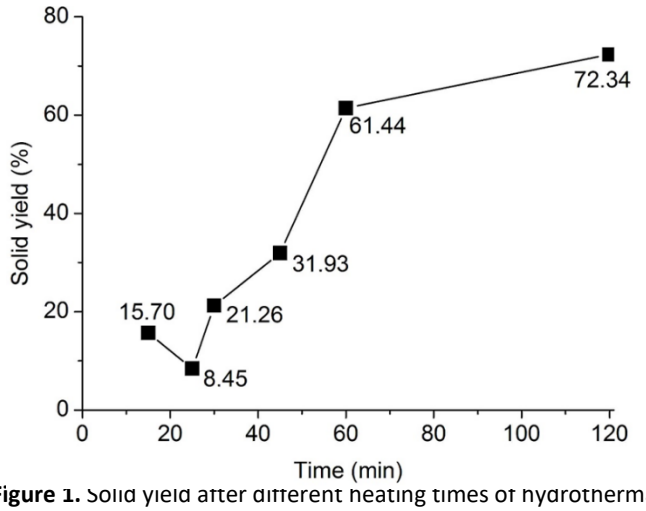

Figure 1. Solid yield after different heating times of hydrothermal treatment.

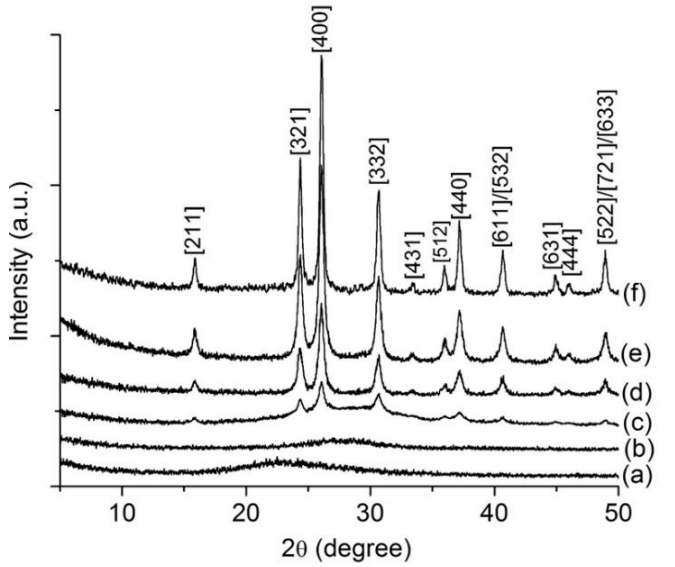

Figure 2. XRD patterns of samples after (a) 15 min, (b) 25 min, (c) 30 min, (d) 45 min, (e) 60 min and (f) 120 min.

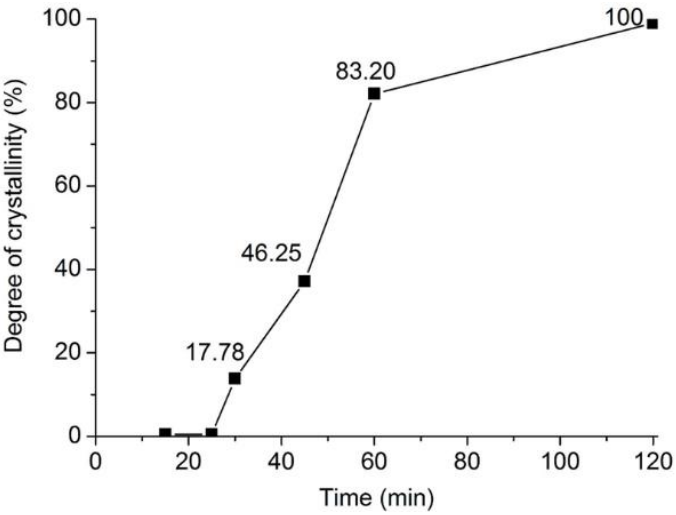

Figure 3. Crystallization rate of solid products after various heating times.

The solid yield kept increasing and reached 31.93% when the hydrothermal heating time was extended to 45 min (Figure 1). All the diffraction peaks corresponding to ANA-type structure were clearly shown with the crystallization rate increasing up to 46.25% (Figure 2d). Further prolonging of the heating time to 60 min shows an enhancement of crystallization rate reaching 83.20%. At this stage, the intensity of all diffraction peaks became stronger and the amorphous phase was no longer dominant in the sample (83.20%). The TEM image also showed that the shape of pollucite was becoming more pronounced where the single nanocrystals of pollucite with trapezohedron shape identical to that of theoretical one, were captured (Figure 4d). As can be seen, amorphous thin layer was still covering the surface of nanocrystals and the nanocrystals were about to dissociate from each other to become an independent single crystal particle (ca. 29 nm) (Figure 4d,e). After 120 min of heating, discrete and fully crystalline Cs-pollucite nanoparticles were obtained (Figure 1–3). As seen, no amorphous

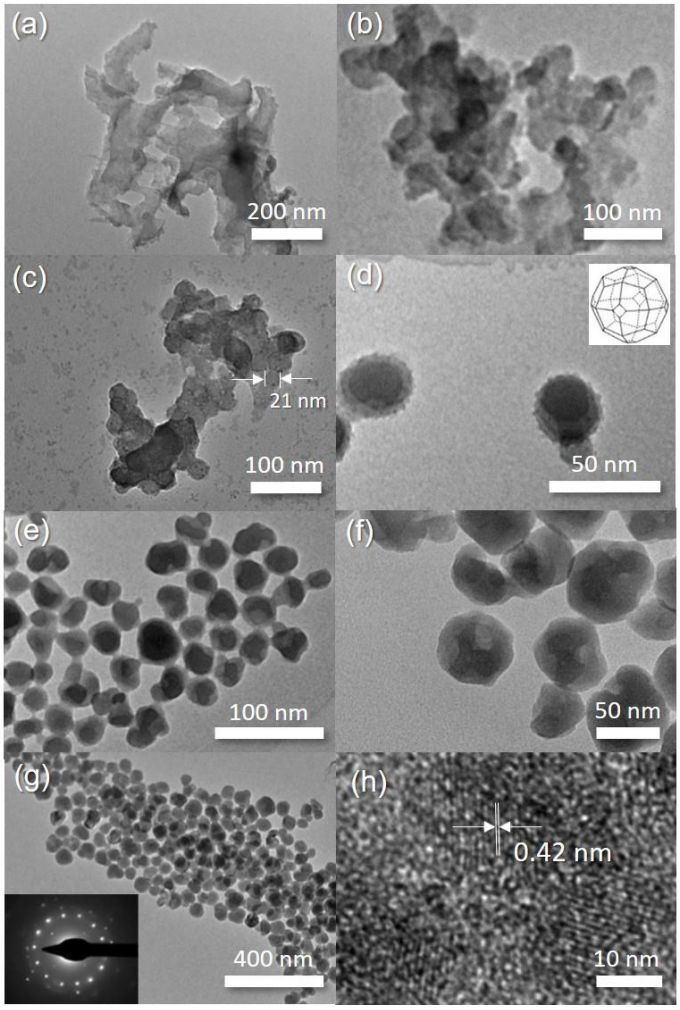

Figure 4. TEM images of samples after (a) 15 min, (b) 25 min, (c) 30 min, (d, e) 60 min and (f, g, h) 120 min. Inset of (d) is the theoretical shape of ANA crystalline solid while inset of (g) is the SAED pattern of sample heated for 120 min.

entities were detected. Instead, the nanocrystals grew further and reached ca. 53 nm (Figure 4f,g). The selected area electron diffraction (SAED) pattern of nanosized Cs-pollucite single crystal viewed along [111] zone axis was also recorded (inset Figure 4g). The SAED pattern showed the nanoparticles to be highly crystalline in nature. The HRTEM image of nanosized Cs-pollucite after 120 min was also captured (Figure 4h). Clear lattice fringes with a spacing of 0.42 nm were observed which corresponded to ANA-type zeolite (theoretical pore size is 0.42 × 0.16 nm^2).[30]

Microscopic study of the formation of nanosized Cs-pollucite

The structural evolution of nanosized Cs-pollucite not only can be explained by their macroscopic properties but also by their microscopic properties. The atomic and molecular spectroscopy analyses were hence used to follow the induction, nucleation and crystallization of pollucite nanocrystals. Figure 5 shows the IR spectra of the samples heated at different time intervals. For the sample heated for 15 min, four IR absorption bands were recorded at 1228, 1114, 800 and 474 cm^{-1} which were attributed to the amorphous aluminosilicate solid (Figure 5a).[7] Two signals

which were assigned to the stretching and bending vibrations of O–H groups of water were also detected at 3470 and 1646 cm^{-1}, respectively.

The IR spectrum pattern changed completely when the sample was further heated to 25 min. For instance, the bands at 474 and 800 cm^{-1}, which were assigned to the bending vibration of TO_4 (T = Si or Al) and symmetric stretching vibration of Si–O–T, respectively, were disappeared (Figure 5b).[34] In addition, the IR bands at 1228 and 1114 cm^{-1} assigning to the internal vibrations of Si–O–T (T = Si, Al) asymmetric stretching mode were red shifted to 1133 and 1053 cm^{-1}. A new IR signal corresponded to Si–OH bending mode was also detected at 863 cm^{-1}.[35] Further heating the precursor to 30 min evidenced the emergence of weak peaks at 769, 725 and 620 cm^{-1} which are characteristic of highly distorted 8-rings subunits present in the pollucite zeolite (Figure 5c).[14] Furthermore, the IR band due to the bending vibration of TO_4 (T = Si or Al) re-appeared again at 447 cm^{-1}. The intensity of these four bands kept increasing with heating time indicating phase transformation of sample from amorphous to crystalline solid (Figure 5c–e). Moreover, the bands at around 1130 and 1020 cm^{-1} were red shifted to lower wavenumbers during crystallization process due to participation and insertion of Al into the pollucite zeolite framework that resulted in a decrease in the Si/Al ratio.

The change in the chemical composition (e.g. Si/Al ratio) was further supported by ICP-OES spectroscopy. As shown in Table 1, the initial Si/Al was 8.11. With increasing the heating time to 25 min, the Si/Al ratio significantly dropped to 4.74 showing the direct participation of Al in the crystallization process. The Si/Al ratio continued to drop but with slower rate to 3.27 after 30 min of heating. The Al content in the solid became almost constant after 60 min and an Si/Al ratio of 2.12 was reached at the end of the crystallization process. On the other hand, the Cs content in the solids showed opposite trend. The initial Cs/Al ratio which was 0.37 increased to 0.76 after 25 min and the Cs content slowly raised and reached to nearly unity after 60 min.

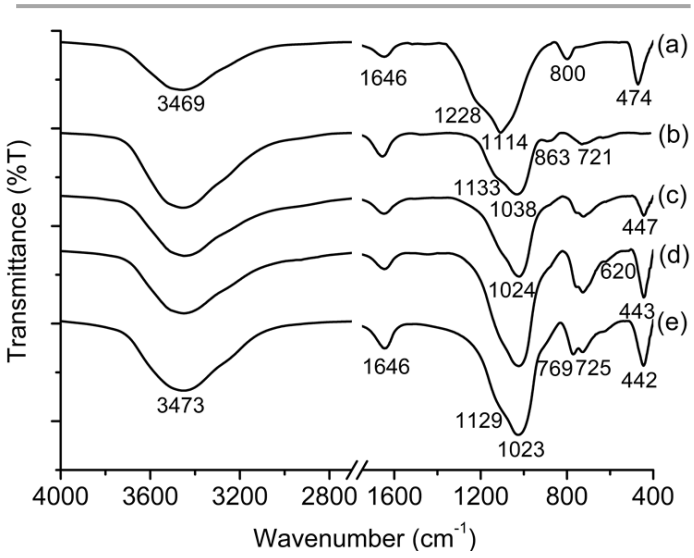

Figure 5. IR spectra of solid products after hydrothermal synthesis for (a) 15 min, (b) 25 min, (c) 30 min, (d) 60 min and (e) 120 min.

Table 1. Si and Al elemental analysis of the solid products obtained after various heating times.

Samples	Si		Al		Cs		Cs/Al ratio	Si/Al ratio
	mg/L	mmol/L	mg/L	mmol/L	mg/L	mmol/L		
15 min	220.7	7.9	26.2	1.0	47.7	0.4	0.37	8.11
25 min	146.6	5.2	29.9	1.1	111.4	0.8	0.76	4.74
30 min	121.5	4.3	35.7	1.3	151.0	1.1	0.86	3.27
45 min	123.2	4.4	49.1	1.8	222.5	1.7	0.92	2.41
60 min	121.7	4.3	53.5	2.0	269.4	2.0	1.02	2.19
120 min	133.4	4.8	60.6	2.2	301.2	2.3	1.01	2.12

^{27}Al and ^{29}Si solid state MAS NMR spectroscopy is a very powerful technique to follow the evolution of zeolites and microporous aluminophosphates.[36-39] Hence, the ^{27}Al solid state MAS NMR spectra of all samples were also recorded. All spectra only indicated a strong peak at 56–59 ppm which was attributed to the Al species in tetrahedral coordination (Figure 6). Hence, the NMR spectroscopy study could prove the direct participation of Al in the formation of pollucite nanocrystals but it did not give much detailed information on the samples with different crystallinity since this tetrahedral Al species is one of the basic building units in both amorphous and zeolite solids. Nevertheless, the $Al_{Tetrahedral}$ peak at ca. –58 ppm became more symmetrical and narrower in the solid sample heated after 30 min, revealing the chemical surrounding of the Al species is becoming more homogeneous when the samples are more crystalline (Figure 6c–e).

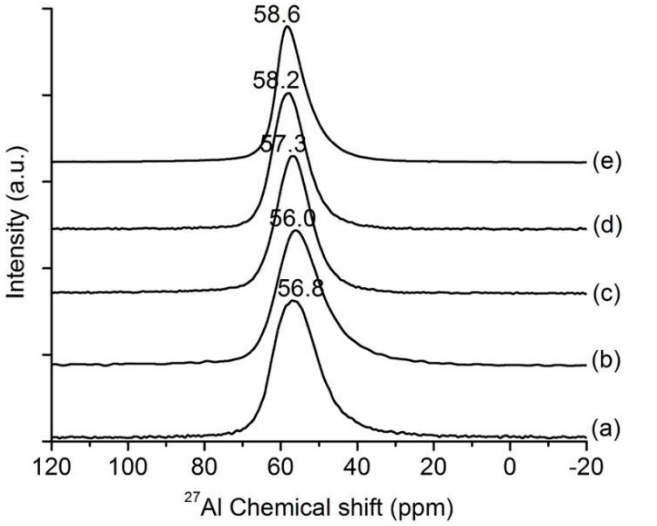

Figure 6. ^{27}Al solid state MAS NMR spectra of samples heated after (a) 15 min, (b) 25 min, (c) 30 min, (d) 60 min and (d) 120 min.

The ^{29}Si MAS NMR spectra for samples heated at different time intervals were also recorded (Figure 7). As shown, it provided more useful information on the chemical environment around the Si atoms in the amorphous, semi- and fully crystalline solids. A broad and non-symmetrical peak was observed from –70 to –120

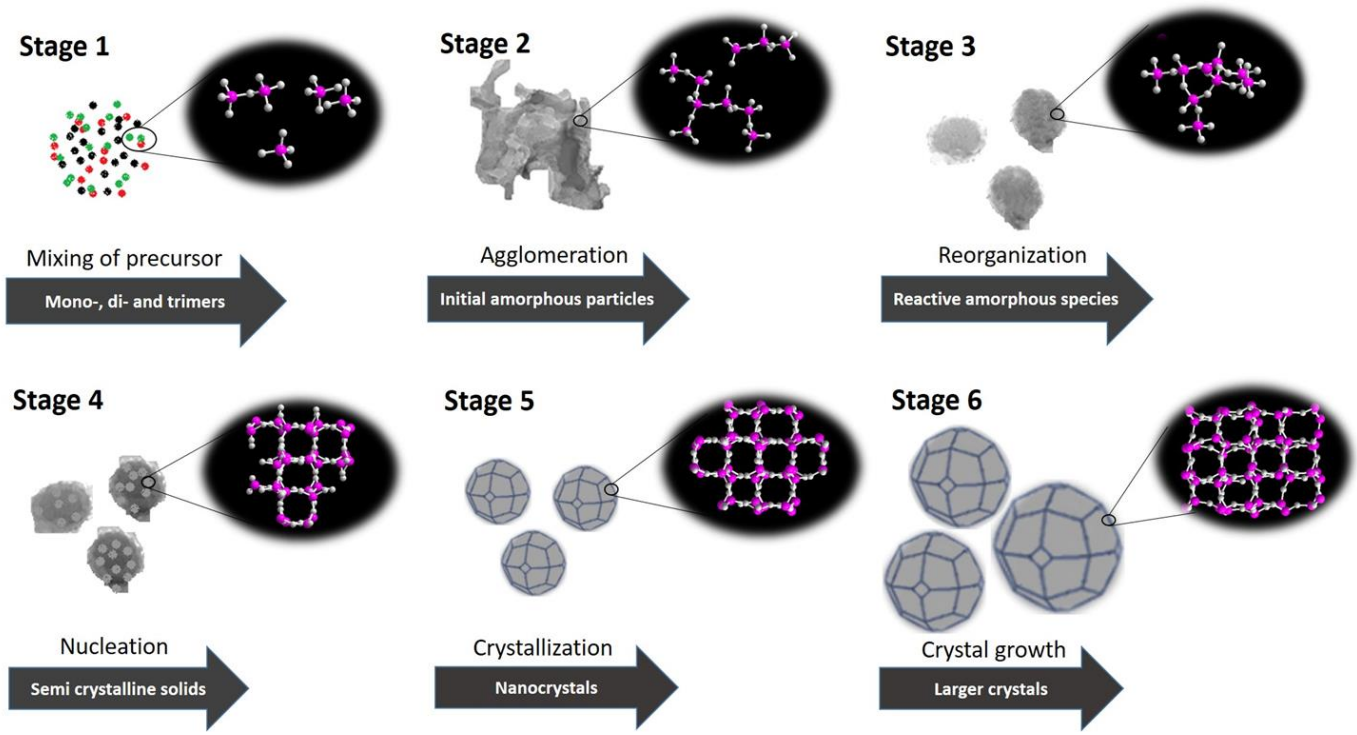

Figure 8. Mechanism of the formation of nanosized Cs-pollucite zeolite. Inset: Framework structure of solid. Pink: Si or Al atom, and white: O atom. Cs atom is not shown.

ppm which could be deconvoluted into 4 peaks (Figure 7a). The peak at –111.4 ppm revealed the presence of non-reacted silica species in the form of $Si(OSi)_4$. The peaks at –102.2 ppm was due to the Q_4 ($Si(OSi)_3(OAl)$) and/or Q_3 ($Si(OSi)_3(OH)$) units, while the peak at -96.8 ppm was attributed to the Q_3 ($Si(OSi)_2(OAl)_2$) and/or Q_3 ($Si(OSi)_2(OAl)(OH)$) units.[36] Another peak observed at -85.5 ppm was due to the Q_2 ($Si(OSi)(OAl)_3$) and/or Q_3 ($Si(OAl)_2(OSi)(OH)$) units. When the sample was heated to 25 min, the peak at -111.4 ppm disappeared (Figure 7b). Only 2 peaks were observed at -88.7 and -96.6 ppm which were due to Q_3 and Q_4 units, respectively. Thus, the NMR investigation was in line with the XRD observation on the phase reorganization of amorphous solid. The symmetry peaks attributing to the unique Si crystallographic sites (Q_1: $Si(OAl)_4$ and Q_2: $Si(OSi)(OAl)_3$) of ANA structure started to appear at ca. –85.5 and –91.0 ppm, respectively after 30 min while another peak due to amorphous Q_3 species, *viz.* ($Si(OSi)_2(OAl)_2$) and/or ($Si(OSi)_2(OAl)(OH)$) groups, was slightly shifted due to the change of the chemical environment in semi-crystalline solids (Figure 7c).[40] The latter peak slowly disappeared with time and only 2 peaks at –85.2 and –92.1 ppm were observed by the fully crystalline sample (120 min) (Figure 7d, e).

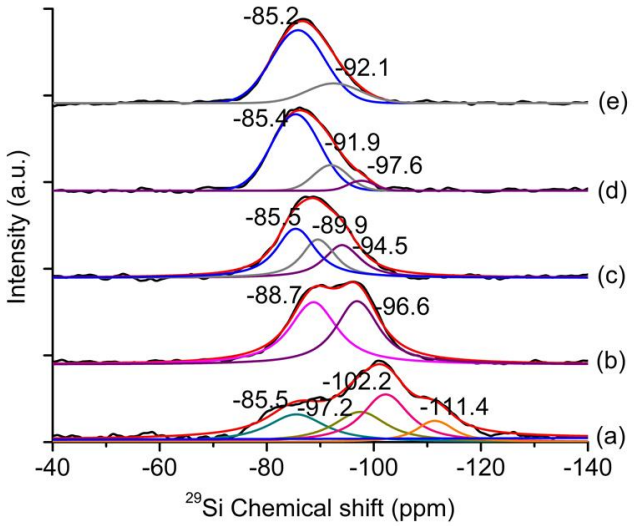

Figure 7. ^{29}Si solid state MAS NMR spectra of samples heated after (a) 15 min, (b) 25 min, (c) 30 min, (d) 60 min and (e) 120 min.

Nucleation process and crystal growth mechanism of nanosized Cs-pollucite

Cs-pollucite zeolite is normally synthesized under extreme condition (200–300 °C, 300–850 bar) where it is inter-converted from natural zeolite and clay. In order to reduce the zeolite crystal size, supersaturation environment is essential to allow nucleation more favourable than crystal growth. Such condition can be achieved by increasing the pH of precursor via increasing the concentration of organic template and metal hydroxide, or reducing the water content.[41] Furthermore, the use of low temperature allows exploration of metastable crystalline phase with open-framework structure and unique properties.[42] In this work, the crystal growth of nanosized Cs-pollucite zeolite is studied in a very reactive hydrosol free of organic template and using more gentle synthesis condition (180 °C, <120 min).

The hydrothermal formation of nanosized Cs-pollucite *via* organotemplate-free pathway is shown in Figure 8 after visual, spectroscopy and microscopy investigations are considered. Initially, the precursor solution is clear upon mixing of both aluminate and silicate solutions even after stirring for 1 h at room temperature. The precursor is then heated at higher temperature (180 °C) to enhance the crystallization rate. In the first 7 min of heating, the precursor solution remains clear and no solid product is formed. In this stage (Stage 1), the Si and Al atoms exist in simple monomeric, dimeric and/or trimeric species forms.

Polymerization starts to take place when the precursor is further heated to 15 min. A cloudy colloidal solution is formed but the solid yield is considerably low (15.70%). The inorganic nutrients are composed of $Si(OSi)_4$, $Si(OSi)_3(OAl)$, $Si(OSi)_3(OH)$, $Si(OSi)_2(OAl)_2$, $Si(OSi)_2(OAl)(OH)$, $Si(OSi)(OAl)_3$ and $Si(OAl)_2(OSi)(OH)$ units which are present, along with free Cs^+ and tetrahedral Al species as well, in the precursor (Stage 2).

When the precursor is further heated to 25 min, the solid yield reduces to 8.45% due to the successive dissolution of initial amorphous entity to generate soluble nutrient species for nuclei growth. The XRD, IR and NMR spectroscopy data also show that amorphous phase reorganization into more reactive amorphous intermediate has taken place (Stage 3). The functional groups and the chemical environment of the solid change significantly. Furthermore, the morphology of the solid changes into 3D solid with irregular shape. At this stage, Al^{3+} and Cs^+ species are actively participated in the construction of amorphous framework where Al^{3+} is incorporated in the solid as Al tetrahedral form while Cs^+ serves as extraframework cation and mineralizer.

Polymerization further takes place at 30 min (Stage 4). The –OH groups bound to Al and Si atoms polycondense to form longer polymer chains containing $Si(OSi)_2(OAl)_2$), $Si(OSi)_2(OAl)(OH)$, $Si(OAl)_4$ and $Si(OSi)(OAl)_3$ units. As a result, more solids precipitate out (solid yield increases). At this stage, Cs-pollucite nuclei, which has almost similar size as the amorphous single particles, are formed and embedded in the bulk amorphous solid as confirmed by XRD and NMR analyses. The crystallization rate speeds up, and the degree of crystallinity is significantly enhanced after 30 min onwards. The nutrients from the amorphous material are gradually consumed and phase transformation from amorphous entity to crystalline particles occurs. After 60 min, the ANA crystalline phase is becoming more dominant (83.20% crystallinity) (Stage 5). Cs-pollucite nanocrystals (ca. 29 nm) with trapezohedron shape are formed but they are still slightly covered by an amorphous thin layer. The nanocrystals are about to dissociate from each other to become an independent single crystal particle. After 120 min of heating, the nutrients in the amorphous entity are completely consumed forming discrete and fully crystalline Cs-pollucite nanocrystals (Stage 6). The crystalline framework of Cs-pollucite is made up of $Si(OAl)_4$ and $Si(OSi)(OAl)_3$ units, producing a high-alumina zeolite (Si/Al ratio = 2.12). The Cs/Al ratio reaches nearly unity because every framework Al species (in tetrahedral form) carrying a negative charge is counter-balanced by a Cs^+ cation. Furthermore, the nanocrystals also grow further (ca. 55 nm) by consuming the nutrients released from the re-dissolution of less stable and smaller crystal domains by the Oswald ripening rule.

Catalytic reaction study in cyanoethylation of amines

Cyanoethylation of dipropylamine was used as a model reaction to investigate the catalytic properties of nanosized Cs-pollucite. The reaction was performed under non-microwave instant heating condition (180 °C) where this heating mode provides very fast and homogeneous heating similar to microwave heating but with different heating mechanism.[43,44] The results show that the nanosolid catalyst is very active with 89.6% conversion after 50 min of heating (Figure 9). The catalytic performance is also compared with two most common homogeneous base catalysts, namely NaOH and KOH. Interestingly, nanosized Cs-pollucite exhibits stronger catalytic activity than KOH (84.8%) and NaOH (79.7%). Thus, it indicates that Cs-pollucite nanocrystals can be used as an eco-friendly and reusable solid base catalyst in organic syntheses.

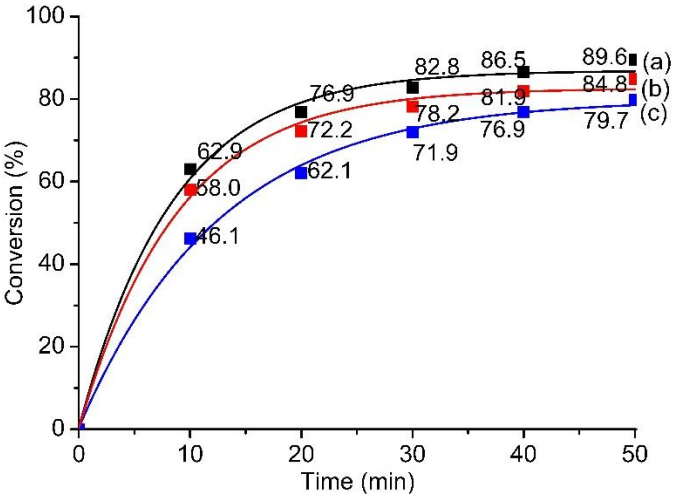

Figure 9. Cyanoethylation of dipropylamine over (a) nanosized Cs-pollucite, (b) KOH and (c) NaOH under non-microwave instant heating at 180 °C.

Conclusion

A detailed macroscopic and microscopic investigation of crystallization of nanosized Cs-pollucite zeolite in organotemplate-free and clear precursor suspension has been reported. The study shows that Cs-pollucite nanocrystals can be easily obtained within 120 min when a very reactive precursor sol is used. The formation of Cs-pollucite zeolite involves mixing of Al and Si simple units, oligomerization of inorganic species to form initial amorphous solid, successive dissolution and polymerization of oligomers to form active amorphous entity (induction), nucleation, crystallization and finally crystal growth. The resulting nanocrystals, which have crystallite size of ca. 55 nm, display trapezohedron morphology. The colloidal stable Cs-pollucite nanocrystals are high-alumina zeolite (Si/Al ratio = 2.12) and the negative charges induced by the presence of Al atoms in the framework are counter-balanced by Cs^+ cations. The synthesis reported in this paper is highly appreciated since colloidal stable Cs-pollucite nanozeolite can be crystallized free of organic template and under mild condition (180 °C, < 120 min, < 25 bar) enables safe and simple scale-up operation. Furthermore, the cyanoethylation of dipropylamine catalytic study concludes that

Cs-pollucite nanocrystals are a potential solid base catalyst and can be an alternative replacement to NaOH and KOH homogeneous base catalysts.

Acknowledgments

The financial support from FRGS (203/PKIMIA/6711642) grant is gratefully acknowledged. The doctoral scholarship from University of Hail, Saudi Arabia is also acknowledged.

References

1 S.M. Al-Jubouri, S.M. Holmes, *Chem. Eng. J.*, 2017, **308**, 476.
2 G. Majano, E.-P. Ng, L. Lakiss, S. Mintova, *Green Chem.*, 2011, **13**, 2435.
3 B. Liu, Z. Chen, J. Huang, H. Chen, Y. Fang, *Micropor. Mesopor. Mater.*, 2019, **273**, 235.
4 E.-P. Ng, D.T.-L. Ng, H. Awala, K.-L. Wong, S. Mintova, *Mater. Lett.*, 2014, **132**, 126.
5 J. Huve, A. Ryzhikov, H. Nouali, V. Lallia, G. Augé, T.J. Daou, *RSC Adv.*, 2018, **8**, 29248.
6 M. Rahimi, E.-P. Ng, K. Bakhtiari, M. Vinciguerra, H.A. Ahmad, H. Awala, S. Mintova, M. Daghighi, F.B. Rostami, M. de Vries, M.M. Motazacker, M.P. Peppelenbosch, M. Mahmoudi, F. Rezaee, *Sci. Rep.*, 2015, **5**, 17259.
7 S.-F. Wong, K. Deekomwong, J. Wittayakun, T.C. Ling, O. Muraza, F. Adam, E.-P. Ng, *Mater. Chem. Phys.* 2017, **196**, 295.
8 S. Mintova, J. Grand, V. Valtchev, *C.R. Chim.*, 2016, **19**, 183.
9 L. Tosheva, E.-P. Ng, S. Mintova, M. Hölzl, T.H. Metzger, A.M. *Chem. Mater.*, 2008, **20**, 5721.
10 T.M.A. Ghrear, S. Rigolet, T.J. Daou, S. Mintova, T.C. Ling, S.H. Tan, E.-P. Ng, *Micropor. Mesopor. Mater.*, 2019, **277**, 78.
11 E.-P. Ng, L. Delmotte, S. Mintova, *Green Chem.*, 2008, **10**, 1043.
12 E.-P. Ng, S.S. Sekhon, S. Mintova, *Chem. Commun.*, 2009, **0**, 1661.
13 G. Majano, K. Raltchev, A. Vicente, S. Mintova, *Nanoscale*, 2015, **7**, 5787.
14 A.G. Mohammad S, N.H. Ahmad, K. Goldyn, S. Mintova, T.C. Ling, E.-P. Ng, Mater. Res. Exp., 2018, **6**, 025026.
15 Y. Kamimura, W. Chailittisilp, K. Itabashi, A. Shimojima, T. Okubo, *Chem. Asian J.*, 2010, **5**, 2182.
16 X. Chen, D. Xi, Q. Sun, N. Wang, Z. Dai, D. Fan, V. Valtchev, J. Yu, *Micropor. Mesopor. Mater.*, 2016, **234**, 401.
17 E.-P. Ng, H. Awala, J.-P. Ghoy, A. Vicente, T.C. Ling, Y.H. Ng, S. Mintova, F. Adam, *Mater. Chem. Phys.*, 2015, **159**, 38.
18 H. Awala, J.P. Gilson, R. Retoux, P. Boullay, J.M. Goupil, V. Valtchev, S. Mintova, *Nat. Mater.*, 2015, **14**, 447.
19 V.P. Valtchev, K.N. Bozhilov, *J. Phys. Chem. B*, 2004, **108**, 15587.
20 J. Kecht, B. Mihailova, K. Karaghiosoff, S. Mintova, T. Bein, *Langmuir*, 2004, **20**, 5271.
21 S. Mintova, N.H. Olson, V. Valtchev, T. Bein, *Science*, 1999, **283**, 958.
22 E.-P. Ng, G.K. Lim, G.-L. Khoo, K.-H. Tan, B.S. Ooi, F. Adam, T.C. Ling, K.-L. Wong, *Mater. Chem. Phys.*, 2015, **155**, 30.
23 M. Tsapatsis, T. Okubo, M. Lovallo, M.E. Davis, *Mater. Res. Soc. Symp. Proc.*, 1995, **371**, 21.
24 Y. Liu, M. Sun, C.M. Lew, J. Wang, Y. Yan, *Adv. Funct. Mater.*, 2008, **18**, 1732.
25 Y.-W. Cheong, K.-L. Wong, T.C. Ling, E.-P. Ng, *Mater. Express*, 2018, **8**, 1.
26 K. Jiao, X. Xu, Z. Lv, J. Song, M. He, H. Gies, *Micropor. Mesopor. Mater.*, 2016, **225**, 98.
27 Y. Ni, A. Sun, X. Wu, G. Hai, J. Hu, T. Li, G. Li, *Micropor. Mesopor. Mater.*, 2011, **143**, 435.
28. T. Kurniawan, O. Muraza, K. Miyake, A.S. Hakeem, Y. Hirota, A.M. Al-Amer, N. Nishiyama, *Ind. Eng. Chem. Res.*, 2017, **56**, 4258.
29 W. Fan, K. Morozumi, R. Kimura, T. Yokoi, T. Okubo, *Langmuir*, 2008, **24**, 6952.
30 IZA-SC Database of Zeolite Structures. http://www.iza-structure.org/ databases/.
31 Y. Yokomori, K. Asazuki, N. Kamiya, Y. Yano, K. Akamatsu, T. Toda, A. Aruga, Y. Kaneo, S. Matsuoka, K. Nishi, S. Matsumoto, *Sci. Rep.*, 2014, **4**, 4195.
32 Y. Chen, Z. Jing, K. Cai, J. Li, *Chem. Eng. J.*, 2018, **336**, 503.
33 S.-F. Wong, H. Awala, A. Vincente, R. Retoux, T.C. Ling, S. Mintova, R.R. Mukti, E.-P. Ng, *Mater. Chem. Phys.*, 2017, **196**, 295.
34 Z. Yan, D. Ma, J. Zhang, X. Liu, X. Han, X. Bao, F. Chang, L. Xu, Z. Liu, *J. Mol. Catal. A: Chem.*, 2003, **194**, 153.
35 B.-Z. Zhan, M.A. White, M. Lumsden, J.M. -Neuhaus, K.N. Robertson, T.S. Cameron, M. Gharghouri, *Chem. Mater.*, 2002, **14**, 3636.
36 I.I. Ivanova, Y.G. Kolyagin. I.A. Kasyanov, A.V. Yakimov, T.O. Bok. D.N. Zarubin, *Angew. Chem. Int.*, 2017, **56**, 15344.
37 A. Aerts, C.E.A Kirschhock, J.A. Martens, *Chem. Soc. Rev.*, 2010, **39**, 4626.
38 S.-F. Wong, H. Awala, A. Vincente, R. Retoux, T.C. Ling, S. Mintova, R.R. Mukti, E.-P. Ng, *Micropor. Mesopor. Mater.*, 2017, **249**, 105.
39 F. Taulelle, M. Haouas, C. Gerardin, C. Estournes, T. Loiseau, G. Ferey, *Colloid Surface A*, 1999, **158**, 299.
40 G. Engelhardt, Solid state NMR spectroscopy applied to zeolites, *Stud. Surf. Sci. Catal.* 2001, **137**, 387.
41 M. Kamali, S. Vaezifar, H. Kolahduzan, A. Malekpour, M.R. Abdi. *Powder Technol.*, 2009, **189**, 52.
42 V.P. Valtchev, K.N. Bozhilov, *J. Phys. Chem. B*, 2004, **108**, 15587.

Micro- and Macroscopic Observations of the Nucleation and Crystal Growth of Nanosized Cs-Pollucite in Organotemplate-free Hydrosol

Eng-Poh Ng,† Aleid Ghadah Mohammad S, Severinne Rigolet, T. Jean Daou, Svetlana Mintova, Tau Chuan Ling

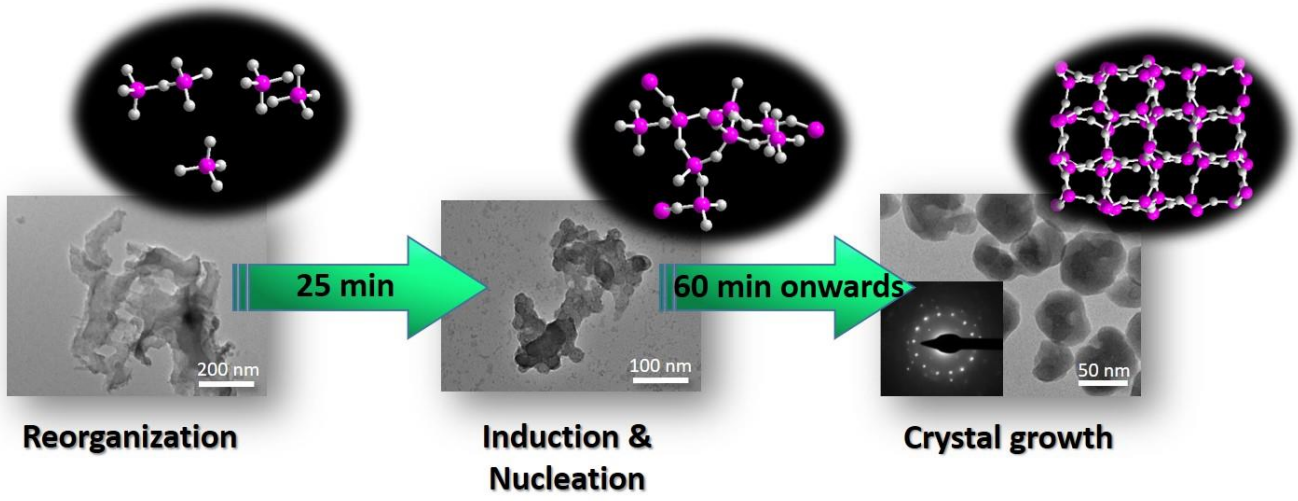

Nucleation and crystal growth of nanosized cesium pollucite zeolite from organotemplate-free hydrosol under mild conditions (low pressure and temperature) are followed and reported.